

ELECTRICAL BREAKDOWN TIME DELAY IN GASES AT LOW PRESSURES

UDC 537.565/.568

Momčilo Pejović¹, Goran S. Ristić¹, Jugoslav P. Karamarković²

¹Faculty of Electronic Engineering, ²Faculty of Civil Engineering and Architecture
University of Niš, Serbia, Yugoslavia

Abstract. *A review of our investigations on the time delay of electrical breakdown in gases at low pressures has been presented in this paper. Statistical analysis of time delay using Laue distributions and histograms of experimental data has been performed. The influence of different parameters (overvoltage, electrodes' temperature and material, glow current) on time delay has been considered. Memory curves have been analyzed and applied to estimate positive ion recombination time, nitrogen atom catalytic recombination time as well as deexcitation time of metastable states in krypton.*

1. INTRODUCTION

It is well known that electrical breakdown in gases does not take place immediately upon applying a definite voltage to the gas-filled tube, but after a corresponding delay. In the first investigations in this field [1-3] the measurements of time delay of electrical breakdown in a gas t_d under defined conditions were carried out, and nothing could be noticed concerning the stochastic character of this phenomenon. A clear picture of this phenomenon was given by Zuber [4] showing that t_d values are subjected to statistical fluctuations and have a definite distributions. Due to the importance of this problem in electroenergetics, very detailed investigations were done by Strigel [5,6]. Wijsman [7] published a detailed analysis of the breakdown probabilities in avalanches.

A problems of breakdown time delay have been investigating in Electronic Industry of Niš, and later in Faculty of Electronic Engineering, University of Niš over the fourth years. The investigations included the influence of many various parameters on time delay: d.c. and a.c. voltage (with various frequencies), work function of cathode material, gas pressures, tube bulb material, tube irradiation, temperature of gas and electrodes, gas flow rate, interelectrode distance, glow current, glow and afterglow periods, etc. One of

Received February 26, 2001

This paper was prepared as Invited lecture for 20th SPIG 2000 but authors were not able to present the paper

the most important result of those investigations is the establishment of a original method for the detection of ions and neutral active states, applicable to the very low concentrations.

There are many definition of time delay of electrical breakdown. One of these is as follows: t_d is the time elapsed from the instant of time when applied voltage reaches the static breakdown voltage U_s to the moment when it start to decrease due to the breakdown in gas-filled tube [6]. The definition of the time delay in our approach is as follows: t_d is the time interval between the moment of application of operating voltage U_w ($U_w > U_s$, where U_s is the static breakdown voltage) to the tube and the moment when the tube current exhibits a detectable discharge.

This paper is dedicated to the investigations of gas breakdown at low pressures, when secondary electron emission (SEE) from the cathode is the main cause of breakdown initiation. At relatively low pressures (up to ≈ 10 mbar) the breakdown mechanisms in gases depend largely on the presence of positive ions and neutral active states, remained from previous discharge.

For many gases the SEE coefficient of the ion impact on cathode is bigger than the corresponding SEE coefficient of neutral active states. But, some exceptions for different combination of gases and cathode materials are observed. The investigation have shown [8] than the coefficient of SEE of the metastable atoms and/or molecules could be either approximately equal with, or slightly large than SEE coefficient of positive ions. For example, the SEE coefficient is 0.023 for metastable atoms and 0.022 for positive ions in the case of argon-filled tubes with tungsten electrodes. The SEE coefficients are 0.071 and 0.065 for the metastable atoms and positive ions, respectively, in argon-filled tubes with molybdenum electrodes [8].

There are few methods available for the detection of metastable atoms or molecules in gases. The optical methods are generally adopted, but they are applicable only in the case of high concentrations ($\approx 10^{11} \text{ cm}^{-3}$) of metastable states [9]. However, these methods do not enable the detection of positive ions and other neutral active states that might be also responsible for SEE. Our investigations [10]-[15] has shown that these particle densities can be very efficient studied by the time delay method. This method is based on the determination of dependence of the mean value of electrical breakdown time delay \bar{t}_d on the afterglow period τ , and this $\bar{t}_d = f(\tau)$ dependence is known as memory curve. The afterglow period τ is the time interval between the voltage turn off in previous and turn on in following discharge. The time delay method enable very efficient separation of the contribution of the positive ions and neutral active states that can be observed to such a low concentration when cosmic rays start to dominate in initiation of breakdown [12,14,15].

2. EXPERIMENTAL DETAILS

The time delay measurements were performed on a gas-filled molybdenum glass tubes with two spherical electrodes made of Al, Pb, Mo, Fe, W, Cu and Au (the shape of the tube is given in [16]). Before the gas was admitted, the tubes were baked out at 350°C and evacuated to a pressure of 10^{-7} mbar in a process similar to that for production of X-ray and other electron tubes. The tubes were than filled with Matheson research grade gases

(N_2 , Ar or Kr) at different pressures (oxygen impurity was contented less than 1 ppm). Before the static breakdown voltages were determined the cathode sputtering with glow current of 0.5 mA was done. The static breakdown voltage U_s was determined from the curves representing the dynamic breakdown voltage U_p versus the rate of the increase of the applied voltage k [17]. The dynamic breakdown voltage U_p was determined in the following manner. A d.c. voltage that is smaller than the expected dynamic breakdown voltage was applied to the tube in advance. After that, at the equal time intervals, the voltage was increased in 1 V steps until breakdown. The rate of the increase of the applied voltage k is defined as the ratio between the voltage step (1 V) and time interval between successive steps. The intersection of $U_p = f(k)$ curve to U_p -axis gives the value of static breakdown voltage U_s .

Besides measurements with cold electrode, some were done with electrode heated up to 400°C. On the basis of Richardson-Dushman's expression [18] one can conclude that thermoelectronic emission was practically excluded under operating conditions. Analysing the problem by Fowler-Nordheim's equation [19] it can be concluded that autoelectronic emission in these experiments could be disregarded.

To eliminate the photoelectron emission, tubes were protected from the light. \bar{t}_d were established from the series that contains at least 100 measurements of t_d . Some tubes were exposed on gamma-rays from radioactive source ^{60}Co , using different values of exposed dose rate, and illumination from nitrogen-filled lamps.

During the experiment, the series of high-voltage pulses that cause the gas breakdown were applied to the tube (Fig. 1). The time interval between two pulses is defined as afterglow period τ . t_g is the constant period during the current i_g flows through the tube. In all measurements t_g was held at 1 s, and it was sufficient to establish saturation of the concentrations of both the ions and neutral active states. The magnitude of voltage pulse is $U_w = U_s + \Delta U$, while $\Delta U/U_s \times \%$ is the fractional overvoltage.

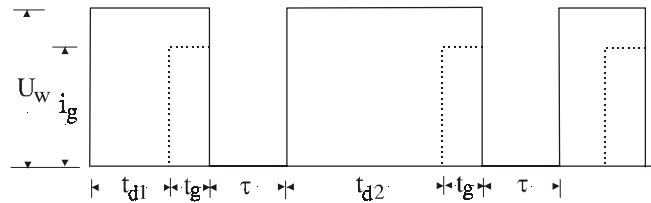


Fig. 1. Measuring cycles: U_w - operating voltage, i_g - glow current, t_{d1} , t_{d2} , ... - time delays, t_g - glow period, τ - afterglow period.

Early measurements of t_d were done by electronic timer (1192 Counter, General Radio) according to the schematic diagram shown in [20]. The manual character of measurement circuit arose the problems since exact settings of glow and afterglow period weren't possible. In the recent years, the measurements were done by system controlled by PC, and schematic diagram of these experimental setup is shown in Fig. 2. It consists of Voltage Supply and Sence (VSS) subsystem, Analog Relaxation Time Setting (ARTS) subsystem and Digital Control Measurement (DCM) subsystem. The VSS subsystem is composed of regulated DC power supply 100–1000 V (20 mA), steady-state current

regulation resistors and sensor resistor for selection of appropriate start-stop measuring level. ARTS subsystem is based on timer 555 and demultiplexer CD 4051, with the primary purpose to establish manual and semiautomatic modes. The DCM subsystem is composed of PC with data acquisition card under control of program for time delay measurement, glow and afterglow time settings (see Ref. [21] for more details).

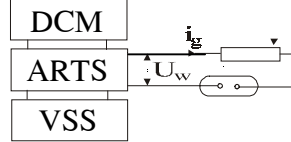


Fig. 2. Block diagram of the experimental setup.

3. DISTRIBUTION OF TIME DELAY

Breakdown time delay t_d has a statistical nature and consists of statistical time delay (t_s) and formative time (t_f), i.e. $t_d = t_s + t_f$. The statistical time delay is the period of the time elapses between the instant of application of an electric voltage in excess of the static breakdown voltage and the arrival of a free electron able to initiate the breakdown process. The time taken from the end of the initiatory lag to the onset of breakdown, characterized by the collapse of the applied voltage as a self-maintained glow, is the formative time [22].

Due to the different physical mechanisms, distributions of statistical time delay and formative time are different. Formative time is determined by avalanche processes and it dominantly has a distribution with small variance, i.e. $\sigma_{t_f} \ll \bar{t}_f$. Consequently, in the case of fixed measurement conditions formative time could be considered as deterministic variable. In contrary, statistical time delay needs more complex model. The process of appearance of the secondary electrons in the vicinity of cathode could be successfully modelled by Poisson random process. It means that the number of created secondary electrons in the observed time interval $(0, t)$ is random variable with Poisson distribution $P(Yt)$, and the distribution of time interval between two subsequent secondary electrons is exponential with the probability density function (PDF)

$$g(t) = Y \exp[-Yt] \quad (1)$$

where Y is the average number of created secondary electrons per time unit (electron yield). In order to obtain the distribution of statistical time delay one has to take into account the fact that every electron is not effective, i.e. the successful avalanche is not produced by every electron. If W is the probability of one electron to cause the breakdown, assuming the independent avalanches [23], PDF of statistical time delay could be expressed as:

$$g(t) = YW \exp[-YW t] \quad (2)$$

where YW is the effective yield i.e. yield of effective electrons.

The distribution of time delay depends on the ratio of t_f and t_s , and three different cases can be noticed:

- (i) $t_f \gg t_s$ In this case time delay is effectively only the formative time $t_d \approx t_f$. Physically it corresponds to the case with very large electron yield Y , when initially electron is produced immediately.
- (ii) $t_f \approx t_s$ Electron yield is smaller and magnitudes of formative time and statistical time are of the same order.
- (iii) $t_f \ll t_s$ Electron yield Y is small enough and t_d has the same statistical nature as t_s , i.e. $t_d \approx t_s$.

Let's analyse the distribution of time delay in the third case. Having in mind small variance of t_f , it is possible to write $t_d = t_s + A$, where $A = f(t_f)$ is the suitable estimation of formative time t_f . Thus, t_d obeys shifted exponential distribution with PDF:

$$g(t) = \begin{cases} 0 & t < A \\ YW \exp[-YW(t - A)] & t \geq A \end{cases} \quad (3)$$

The cumulative distribution function (CDF) is defined as the probability that breakdown takes place before the moment of time t

$$F(t) = P\{t_d < t\} = \int_A^t g(t') dt' = 1 - \exp[-YW(t - A)], \quad (4)$$

while the probability that breakdown will appear after the moment of time t has the form

$$R(t) = 1 - F(t) = P\{t_d > t\} = \int_t^{+\infty} g(t') dt' = \exp[-YW(t - A)]. \quad (5)$$

Mean value \bar{t}_d and standard deviation σ are:

$$\bar{t}_d = \int_A^{+\infty} t g(t) dt = A + \frac{1}{YW} = A + \bar{t}_s \quad (6)$$

$$\sigma = \left\{ \int_A^{+\infty} (t - \bar{t}_d)^2 g(t) dt \right\}^{1/2} = \frac{1}{YW} = \bar{t}_d - A. \quad (7)$$

Eqn. (7) shows that formative time can be estimated as

$$t_f = A = \bar{t}_d - \sigma. \quad (8)$$

This estimation method is known as moment method.

Since $R(t)$ can be expressed as

$$R(t) = \frac{n(t)}{N} = \exp\left[-\frac{t - A}{\bar{t}_s}\right], \quad (9)$$

where $n(t)$ is the number of t_d values greater than actual time t and N is the total number of measured t_d values, it is obvious that eqn. (9) enables appropriate visual interpretation of time delay distribution. Namely, plot of $\ln(n/N)$ vs. t represents linear graph, known as Lauegram, and formula (9) is known as Laue distribution [22], regarding the pionir work

[24] of von Laue.

The points of Lauegram obtained on the basis of t_d measurements enable the estimations of t_f and \bar{t}_s . If the linear graph is plotted through this points using some best fit method, \bar{t}_s is the slope of $\ln(n/N)$ vs. t , while t_f can be estimated from the intersection of that graph with the time axis. To obtain an adequate accuracy in evaluation of \bar{t}_s and t_f it is essential N to be big, since the accuracy increases as $\sqrt{1/N}$ [22].

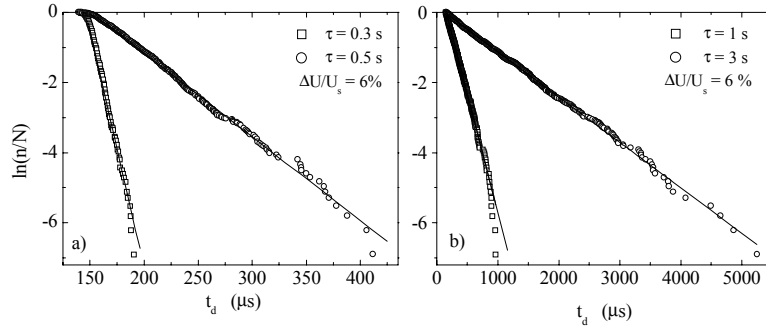


Fig. 3. Laue distributions of t_d for different afterglow periods.

Fig. 3 shows the Laue distributions of 1000 t_d values for afterglow periods from 0.3 to 3 s and overvoltage of 6% for nitrogen-filled tube at 1.3 mbar [13]. Theoretical fits are obtained by the least-square method. The insignificant discrepancy of experimental points from theoretical lines in Fig. 3b indicates the validity of Laue distribution. The same conclusion could be taken for the results shown in Fig. 3a, but the observed knees of the experimental points for small values of t_d could create suspicion. To explore this question, it is useful to plot histograms and fitted corresponding PDF's. This is shown in Fig. 4 for three values of relaxation times τ . Fitting was done in the manner that parameter A in (9) has been estimated as $t_{d \min}$, and after that \bar{t}_s has been obtained from the least-square fit of the function $1 - F(t_d - t_{d \min})$. The results in Fig. 4 show the validity of t_d exponential distribution for $\tau = 1$ s, since the exponential distribution density very precisely fits t_d histogram. On the other hand, for $\tau = 0.3$ and 0.5 s exponential distribution for t_d does not hold. It means that a group of lower t_d values significantly disturbs

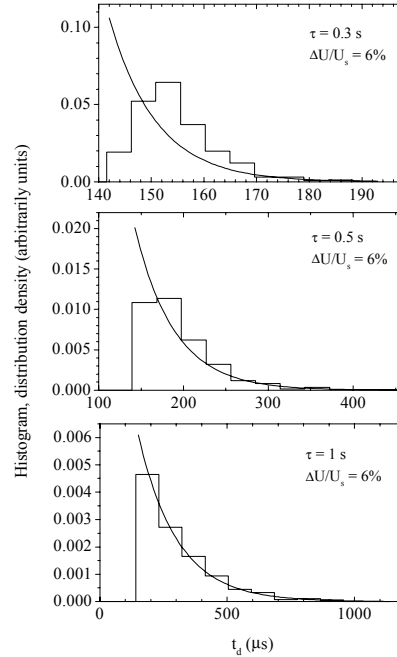


Fig. 4. Histograms and fitted distribution densities of t_d for different afterglow periods.

exponential distribution. It can not be clearly seen from Lauegram (Fig. 3.a), where only a slight discrepancies from the fitted line in low t area can be observed. The reason for the disturbance of exponential distribution is the fact that $\tau = 0.5\text{s}$ and $\tau = 0.3\text{s}$ lay in the transitional region (ii), where physical mechanism for breakdown initiation starts to change.

Fig. 5 shows comparison of different estimations of formative time vs. afterglow period τ . Beside the moment method and estimation from Lauegram mentioned before, third estimation of t_f is minimum t_d value in the set of measured values. This method is based on the fact that shifted exponential distribution (3) is strongly asymmetric and monotonically decreasing, and, consequently, $\lim_{N \rightarrow \infty} \epsilon = 0$, where $\epsilon = t_{d \min} - A$.

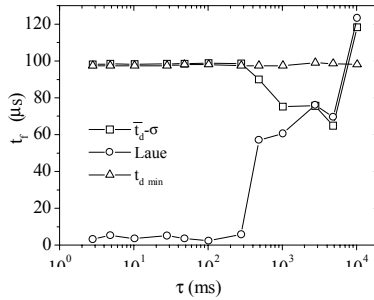


Fig. 5. Estimated formative times with three different methods.

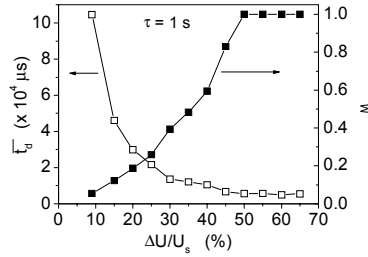


Fig. 6. Time delay mean value \bar{t}_d and breakdown probability W versus overvoltage $\Delta U / U_s$ for krypton-filled tube.

Fig. 5 shows that for small τ , t_f estimated from Lauegram deviates from those obtained by other two methods. Such behaviour is expected since for small τ , t_d lies in areas (i) and (ii), where exponential distribution for t_d is not valid. Agreement of moment method estimation with minimum value could be addressed to the fact that in these areas σ is very small. For bigger τ shifted exponential distribution for t_d is established and moment method and Lauegram t_f estimations give approximately the same results, different from the minimum value. Since change of formative time with the increase of τ is not expected, it could be concluded that those two estimations become rough, and unreliable.

The microscopic breakdown probability W (probability that a secondary electron will lead to the successful avalanche) can be also estimated from the time delay measurements. If \bar{t}_d saturates with the increase of applied voltage, and if a voltage independent yield is assumed, then, neglecting A in (6), it follows [25]

$$W(\Delta U / U_s) = \frac{\bar{t}_{d \text{ sat}}}{\bar{t}_d(\Delta U / U_s)}, \quad (10)$$

where $\bar{t}_{d \text{ sat}}$ is the saturation value of \bar{t}_d . This estimation obtained for krypton-filled tube with pressure $p = 2.7$ mbar is shown in Fig. 6. It is worth to note that this estimation for W is restricted in the area where W is not far away from unity. If $W \ll 1$ the assumption of independent avalanches starts to fail and the whole model described with the equation (2) becomes questionable [23].

4. INFLUENCE OF DIFFERENT EXPERIMENTAL PARAMETERS ON TIME DELAY

Time delay depends on many various experimental parameters. One of the most important is applied voltage, i.e. its excess over static breakdown value (overvoltage). \bar{t}_d vs. $\Delta U/U_s$ dependence exhibits monotonically decreasing behaviour. The analysis of this behaviour will be done in the subsequent text.

Dependences of mean value of time delay on the overvoltage for pressure of 1.3 mbar and afterglow periods of 50 ms, 0.5 s and 1 s, are shown in Fig. 7 [13]. The decrease of the particular curve in Fig. 7 can be explained in a different way. For $\tau = 50$ ms SEE is dominantly induced by positive ions (see next section), and electron yield Y is large enough to give $t_s \ll t_f \rightarrow t_d \approx t_f$. Lower values for \bar{t}_d (i.e. t_f) for low overvoltage values, can be attributed to lower values of electron ionization coefficient. As the overvoltage increases, electrons get a greater amount of kinetic energy between the collisions, their ionization coefficient increases exponentially [26] and t_f falls to its minimum value. In the case of lower electron ionization coefficient, t_f depends on rate of electrons that produce avalanche. This can be seen from Fig. 8 [13], where the \bar{t}_d curves as a function of overvoltage $\Delta U/U_s$ for two values of glow current and $\tau = 50$ ms are shown. Namely, higher glow current produces higher ion number density and consequently, Y increase, decreasing t_d .

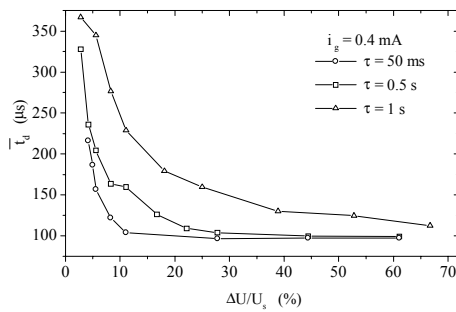


Fig. 7. Time delay mean value \bar{t}_d versus overvoltage $\Delta U/U_s$ for different afterglow periods.

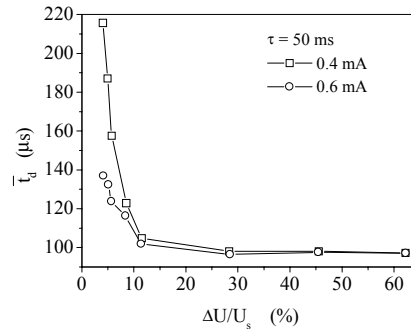


Fig. 8. Time delay mean value \bar{t}_d versus overvoltage $\Delta U/U_s$ for different glow currents.

After $\tau = 1$ s, [13] positive ions have been recombined, Y is reduced, and the corresponding curve decrease (Fig. 7) is the consequence of the increase of probability for an electron to cause the breakdown (W) through the whole overvoltage range, as well as the increase of ionization coefficient for low voltage values. For $\tau = 0.5$ s, the value of Y is not great enough to produce itself $t_d \approx t_f$, but this condition is reached with the increase of overvoltage when W also increases.

The effect of illumination by nitrogen-filled lamps on nitrogen-filled tube at 1.3 mbar is shown in Fig. 9 [27]. As it can be seen the \bar{t}_d values are considerably smaller in the case with illumination lamp than in the case without them, for all values of overvoltage.

This is opposite to the results obtained in [28] where it was shown that the time delay is greater in the case with illumination lamp. Our results show that the light from the illumination lamps does not influence the active states created in the gas during the discharge (i.e. the quenching of $N_2(A^3\Sigma_u^+)$ states) as was concluded in [28, 29]. We consider that the light induces the production of additional secondary electrons from the cathode by photoemission. These released electrons increase the probability of breakdown in gas, leading to a decrease of time delay for the same values of overvoltage.

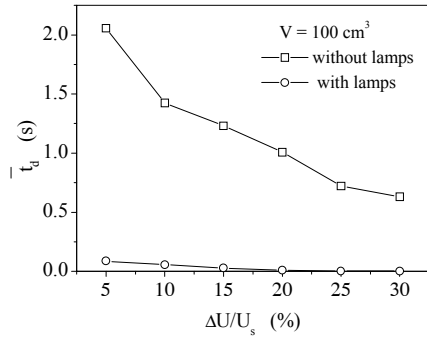


Fig. 9. Time delay mean value \bar{t}_d versus overvoltage $\Delta U/U_s$ with and without the lamp.

electrode material. Mean values of time delay as a function of difference between the applied voltage and the static breakdown voltage ($U_w - U_s$) for nitrogen-filled (7 mbar) tube and different electrode materials at $\tau = 10$ s are shown in Fig. 11 [16]. The obtained results confirm that \bar{t}_d value increases with increase of electrode material work function for given value of $U_w - U_s$ (the work function of Al, Pb and Mo are 3.74, 4.02 and 4.63 eV, respectively [31]) as the consequence of lowered electron yield.

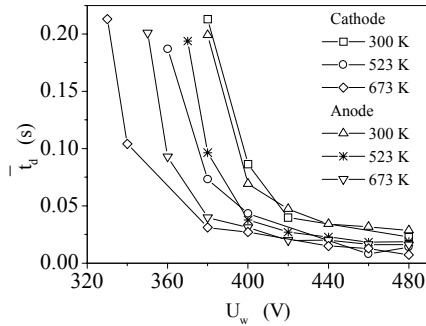


Fig. 10. Time delay mean value \bar{t}_d versus overvoltage $\Delta U/U_s$ for different electrodes' temperatures.

The temperature of electrodes influences breakdown time delay. Fig. 10 shows dependence of $\bar{t}_d = f(U_w)$ for argon-filled tube at 13.3 mbar and $\tau = 10$ s [30]. The static breakdown voltage (U_s) were found as 312, 308 and 305 V d.c. at cathode temperatures of 300, 525 and 673 K, respectively. On the basis of obtained results it can be concluded that for a given value of U_w , \bar{t}_d decreases when the electrode temperature increases. This decrease is the consequence of the increase of the thermal velocity of metastable states remained from the previous discharge due to the higher temperature in interelectrode spaces.

The next investigated parameter is electrode material. Mean values of time delay as a function of difference between the applied voltage and the static breakdown voltage ($U_w - U_s$) for nitrogen-filled (7 mbar) tube and different electrode materials at $\tau = 10$ s are shown in Fig. 11 [16]. The obtained results confirm that \bar{t}_d value increases with increase of electrode material work function for given value of $U_w - U_s$ (the work function of Al, Pb and Mo are 3.74, 4.02 and 4.63 eV, respectively [31]) as the consequence of lowered electron yield.

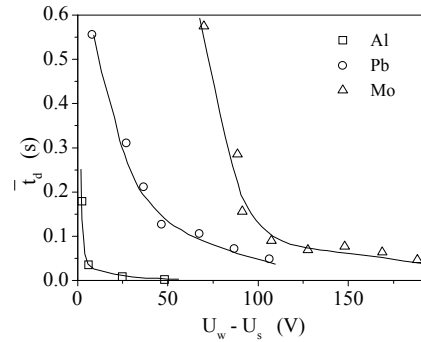


Fig. 11. Time delay mean value \bar{t}_d versus overvoltage $\Delta U/U_s$ for different electrode materials.

We also investigated the influence of glow current on breakdown time delay. Fig. 12 gives \bar{t}_d curves versus the discharge current i_g in nitrogen-filled tubes at pressures of 1.3, 4.0 and 13.3 mbar, respectively and $\tau = 10$ s [32]. As it can be seen, in the low current range \bar{t}_d decreases with increase of current i_g , passes a minimum, and then begins to increase. The minimum value depends on the gas pressure in the tube. The minima of the curves for pressures of 1.3, 4.0 and 13.3 mbar occur approximately at current of 14, 140 and 1100 μ A, respectively. It can be also noticed that the minimum moves toward higher \bar{t}_d values with increase of the pressure. The appearance of minima in these curves indicate the existence of optimum value of glow current that correspond to the maximum number density of created neutral active states during the discharge.

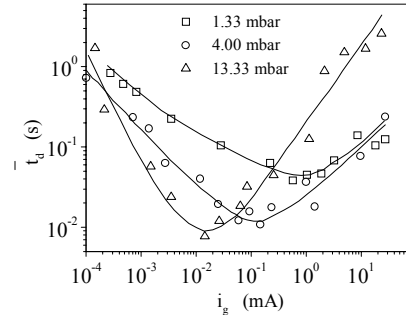


Fig. 12. Time delay mean value \bar{t}_d versus glow current i_g for different pressures.

5. MEMORY CURVES

As it was mentioned, the basis of the time delay method is to provide the memory curve that represents the dependence of \bar{t}_d on τ . The shapes of memory curves are similar for all gases. It can be concluded that they consist of three regions (Fig. 13). In the first of them, the curve has a plateau and the positive ions are responsible for the breakdown initiation. Since the ions have the high drift velocities and reach to the cathode almost instantly after the application of the voltage, releasing the secondary electrons, the breakdown probability almost does not depend on ion concentration and \bar{t}_d values are small. Namely, the production of the electrons is very high and the time delay is approximately equal to the formative time (\bar{t}_d). Considering this region, the recombination time of ions can be determined as the plateau length. When the ion concentration becomes very low, the memory curve begins to increase, entering the second region, in which the neutral active states remained from the previous discharge are responsible for electrical breakdown. For higher τ values the memory curve saturates when the concentration of long-living neutral active states becomes very low, and, in this case, cosmic rays begin to dominate in the initiation of breakdown, resulting in the approximately constant \bar{t}_d values. The time elapsed to the beginning of the saturation estimates the lifetime of particular neutral active state (e.g. atoms, metastables,...). The attempt of the modelling of the kinetics of the neutral active states in nitrogen has been performed and the fittings of

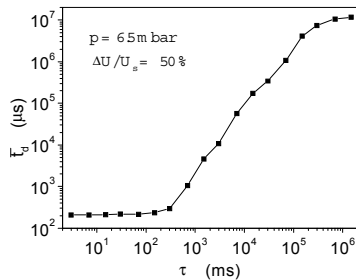


Fig. 13. Memory curve of nitrogen.

of long-living neutral active states becomes very low, and, in this case, cosmic rays begin to dominate in the initiation of breakdown, resulting in the approximately constant \bar{t}_d values. The time elapsed to the beginning of the saturation estimates the lifetime of particular neutral active state (e.g. atoms, metastables,...). The attempt of the modelling of the kinetics of the neutral active states in nitrogen has been performed and the fittings of

some parts of the memory curves have been given [25, 33]. Namely, the corresponding partial differential equations can be given on the basis of processes occurred in nitrogen-filled tube (each term in them represents one of processes in the gas), and the solutions enable fitting of the memory curves.

Here, the analysis of the memory curves obtained by the nitrogen-filled tube will be firstly done. As it was above mentioned, at the relatively low pressures (up to 10mbar), the probability for the breakdown in nitrogen largely depend on the concentration of either the ions or the neutral active states, produced in the previous discharge, depending on the region of memory curves. Since the ions have a relatively short lifetime (to 300ms [34]), the breakdown after longer afterglow period is due to SEE created in recombination processes of neutral active states. These states, called "activated nitrogen", include vibrationally excited molecules, electronically excited metastable states as $N_2(A^3\Sigma_u^+)$ and nitrogen atoms [35].

Many investigations have shown that effective lifetime of $N_2(A^3\Sigma_u^+)$ metastable states, produced in the previous discharge in gas phase, is determined by quenching processes. These metastable states can be quenched in collision with nitrogen atoms [36], other $N_2(A^3\Sigma_u^+)$ metastable states (reaction of energy pooling) resulting $N_2(B^3\Pi_g)$ and $N_2(C^3\Pi_u)$ [37, 38], neutral molecules [39] and wall of tube [40]. Else, the $N_2(A^3\Sigma_u^+)$ state has a very small effective lifetime (in the order of millisecond [33, 41]) and cannot influence the breakdown in later afterglow periods. Since the effective lifetime of N atoms, produced in the previous discharge, is several hours [42], these atoms play dominant role in releasing of secondary electrons from the cathode in nitrogen-filled tubes after long afterglow periods. Namely, a part of N atoms recombines at the cathode (by catalytic recombination processes), giving $N_2(A^3\Sigma_u^+)$ metastable states and producing secondary electrons [41, 43]. If voltage is applied, these electrons can cause the electrical breakdown.

The memory curve for overvoltage $\Delta U/U_s = 50\%$, obtained by nitrogen-filled tube (6.5 mbar) and iron cathode, is presented in Fig. 13. As can be seen, in the τ interval from 3 to 200 ms the curve has the plateau, i.e. the ions are responsible for the breakdown in these region ($\bar{\tau}_d$ very slightly depends on τ). After the positive ions recombination ($\tau > 300$ ms) the SEE is initiated solely by nitrogen atoms through their surface-catalysed recombination to N_2 . For the higher values of τ , the saturation of the memory curve appears, since the concentration of the atoms is very low and the cosmic rays with approximately constant flux become responsible for the breakdown.

The very important parameters that determine the shape of the memory curves are cathode material, gas type, overvoltage, pressure and additional ionization. In the Fig. 14 the dependence of $\bar{\tau}_d$ on cathode material for the nitrogen-filled tube is presented [44]. As can be seen, the curves intersect themselves for the $\tau \approx 400$ ms, when the secondary electrons are stil solely released from the cathode by the positive ions. After that, the nitrogen atoms are responsible for the secondary electron emission, and the $\bar{\tau}_d$ values are greater for the bulk copper cathode than for gold plated cathode. This difference can be explained by different adsorption ability of cathode materials, according to adsorption model [45]. Namely, the adsorbed layer of N atoms covered by a pseudo-layer of N_2 molecules is formed on metal surface, decreasing the probability of secondary electron

emission through adsorbed layers. Since the N atoms are more adsorbed on the copper, the probability of secondary emission from copper is considerably smaller than from gold plated cathode.

The time delay method can also be used for other gases. In Fig. 15 the dependence of memory curve on overvoltage for the krypton at 2.6mbar is shown [15]. \bar{t}_d increases with the increase of $\tau \approx 100$ s, and after that, the curves reach the saturation for all overvoltage. The curves show the saturation since the concentration of metastable states decreases very much and cosmic rays begin to dominate in initiation of breakdown. It can also be seen that in the late afterglow, when the breakdown is initiated by secondary electrons induced from the cathode by metastables, the time delay decreases with the overvoltage increases. This is expected, since the probability for appearance of the avalanche that leads to breakdown increases with the overvoltage increase.

Since \bar{t}_d is insignificantly changed up to $\tau \approx 30$ ms, especially for overvoltages of 50 and 100% (see Fig. 15), it can be supposed that the positive ions have dominant role in secondary emission of the electrons from the cathode in this region, and that their recombination time is about 30 ms.

For $\tau > 30$ ms, the ions are recombined during the afterglow period, and the SEE from the cathode is mostly triggered by metastables, which deexcite themselves at the cathode surface. Since these curves reach the saturation for $\tau \approx 100$ s, it can be concluded that the metastable lifetime in krypton at this pressure is about 100 s. Time-of-flight method has shown [46] that lifetimes of metastables states in krypton are >1 s, while theoretical calculation gives $\tau(^3P_2$ nonradiative lifetime as 85.1 s [47].

Influence of the gas pressure on the shape of memory curve is presented in Fig. 16 [48]. It can be estimated that the recombination time of positive ions in argon at pressure of 0.66 mbar is about 150 ms and at pressure of 66 mbar is shorter than 3 ms, meaning that the recombination rate of positive ions increases with the pressure. As it can also be seen, the saturation of the memory curves appears earlier in the case of higher pressure, meaning that the deexcitation rate of metastable states increases with the pressure. Namely, the mean free path of metastable states remained from previous discharge decreases with the increase of gas pressure increasing the possibility for their deexcitation [49].

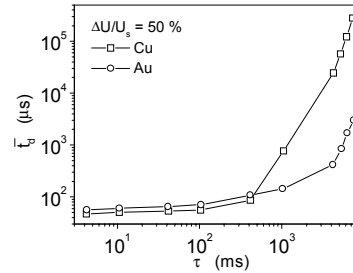


Fig. 14. Memory curves of nitrogen for different cathode materials.

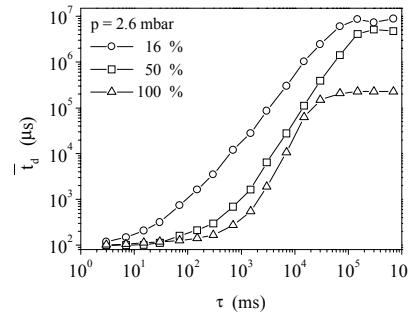


Fig. 15. Memory curves of krypton for different overvoltages.

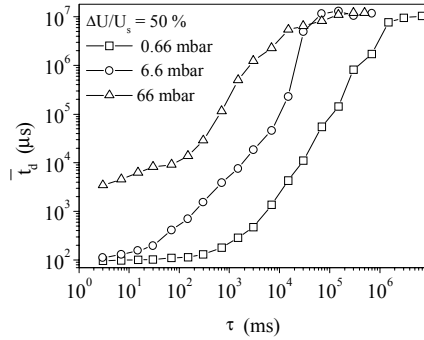


Fig. 16. Memory curves of argon for different pressures.

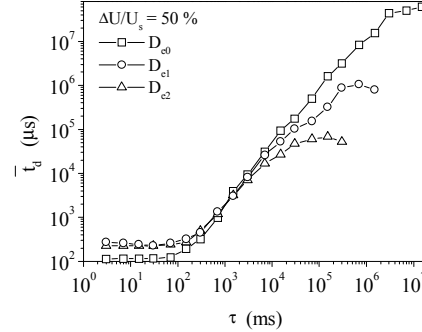


Fig. 17. Memory curves of nitrogen for different exposed dose rates.

Based on the memory curve dependence it is also possible to detect Compton's electrons from the cathode induced by γ -rays present in gas tube. The memory curves for overvoltage $\Delta U/U_s = 50\%$ in the case with and without the irradiation (two different exposed dose rates $RD_{e1} = 2.1 \cdot 10^{-11} \text{ Ckg}^{-1}\text{s}^{-1}$ and $RD_{e2} = 6.5 \cdot 10^{-10} \text{ Ckg}^{-1}\text{s}^{-1}$) for the nitrogen-filled tube at 1.33 mbar are shown in Fig. 17 [14]. As can be seen, for τ interval from 3 to 200 ms, the curves have plateaus and there are the differences in \bar{t}_d values in the case with and without radiation (t_d values are greater in the case of radiation), while they do not exist between two exposed dose rates. Namely, the external ionizing radiation decreases the probability for the electrical breakdown releasing the Compton's electrons from cathode in interelectrode space that increase the recombination of ions decreasing their efficiency to arrive to the cathode.

For the τ interval from 200 ms to 6 s, the nitrogen atoms are responsible for breakdown, and there aren't the significant differences between memory curves since atom concentrations are very high. For $\tau > 6$ s, clear differences in \bar{t}_d values appear, and the influence of radiation can be separated. Namely, the concentration of N atoms sufficiently decreases, and secondary electrons released by gamma photons begin to dominate in initiation of breakdown. In the case without radiation, the saturation begins at $\tau = 3000$ s, and after that the breakdown is caused by electrons created by cosmic rays, since the concentration of N atoms is greatly decreased. In the case with irradiation, the \bar{t}_d is lower for the exposed dose rate of RD_{e2} , because the production in unit time of the secondary electrons released from the cathode is higher than for RD_{e1} . The curve reaches saturation because this production is approximately constant for a given exposed dose rate.

The influence of an additional ionization on other gases is also very emphasized. In

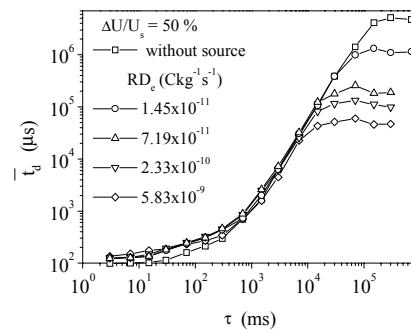


Fig. 18. Memory curves of krypton for different exposed dose rates.

Fig. 18 the memory curves obtained by the krypton-filled tube exposed to the ionizing radiation are shown [15]. The behaviour is very similar to the memory curves in Fig. 17. The values of τ for which the saturations appear increase with the decreases of radiation dose rate, and t_d values are lower for the higher dose rates. These results show that these tubes can be used as the very sensitive sensor of ionizing radiation in some τ intervals, using the memory curves.

6. CONCLUSIONS

Overvoltage is experimental parameter with strong influence on time delay. It has been shown that time delay decreases with increase of overvoltage for small overvoltages and becomes approximately constant after some value of overvoltage. This behaviour does not depend on the type of breakdown initiation (positive ions and neutral active states or only neutral active states initiation). The light originated from discharge in nitrogen filled lamp induces decrease of time delay in nitrogen-filled tube due to the increase of SEE. This results are in contradiction with results shown in [28, 29] where nitrogen-filled lamp illumination increases time delay due to quenching $N_2(A^3\Sigma_u^+)$ metastable states. Decrease of time delay with the increase of temperature in argon is dominant for lower values of working voltage. This decrease is consequence of the increase of the thermal velocity of metastable states remained from the previous discharge due to the higher temperature in interelectrode space.

Time delay decreases with the increase of cathode material working function as the consequence of the lowered electron yield in the interelectrode space. It has been shown that the value of glow current where time delay has its minimum value increases with the decrease of nitrogen pressure in the tube. The appearance of minimum t_d value for certain current value is the consequence of maximum nitrogen atom concentration established in discharge.

The influence of positive ions and influence of neutral active states remaining from previous discharge on initiation of subsequent breakdown have been performed on the basis of memory curves for nitrogen and krypton filled tubes. Using these curves it is also possible to estimate positive ions recombination time, nitrogen atom catalytic recombination time and krypton metastable states deexcitation time. It has been shown that all of this time values depend on gas pressure, i.e. decrease with increase of pressure, which is in agreement with literature data obtained with different methods. Nitrogen atom catalytic recombination time and argon and krypton metastable states deexcitation time for low pressures are bigger than ones from the literature. This can be explained with the fact that time delay method (recording of memory curves) is few orders of magnitude more sensitive comparing with optical methods. On the basis of memory curves it is possible to detect very efficiently Compton's electrons from the cathode induced by gamma photons originated from radioactive source. It shows that the gas filled tube can be used as very sensitive sensor of low dose gamma-rays.

REFERENCES

1. G. Janmann, *Ann. Chemie Phys. (Wiedemann'sche Annalen)* **5** (1895).
2. E. Warburg, *Ann. Chemie Phys. (Wiedemann'sche Annalen)* **9** (1896) 1.
3. E. Warburg, *Ann. Chemie Phys. (Wiedemann'sche Annalen)* **11** (1897) 385.
4. K. Zuber, *Ann. Phys.* **76** (1925) 231.
5. R. Strigel, *Wissenschaftliche Veröffentlichungen and den Siemens Werken* **11** (1932) 52.
6. R. Strigel, *Elektrische Stossfestigkeit*, Springer, Berlin (1939).
7. R. A. Wijzman, *Phys. Rev.* **75** (1949) 833.
8. D.V. Razevig and M.V. Sokolova, *Raschet nachalnyh i razryadnyh napryadzeniy gazovyh promedzutkov*, Energia, Moskva (1977).
9. G. Cernogora, L. Hochard, M. Touzeou and C. M. Ferreira, *J. Phys. B: At. Mol. Phys.* (1981) 2977.
10. M. M. Pejović, B.J. Mijović and Dj.A. Bošan, *J. Phys. D: Appl. Phys.* **16** (1983) L149
11. M.M. Pejović, B.J. Mijović and Dj.A. Bošan, *J. Phys. D: Appl. Phys.* **17** (1984) 351
12. M. Pejović, B. Mijović, *J. Tech. Phys.* **58** (1988) 2124 (in Russian).
13. M. M. Pejović, J. P. Karamarković and G. S. Ristić, *IEEE Tran. Plasma Sci.* **26** (1998) 1733.
14. M. M. Pejović, G. S. Ristić, *Rev. Sci. Instr.* **7** (2000) 2377.
15. M.M. Pejović and G.S. Ristić, *J. Phys. D: Appl. Phys.* **33** (2000) 2786
16. M.M. Pejović, Dj. A. Bošan and Dj. M. Krmpotić, *Contribution to Plasma Physics* **21** (1981) 211.
17. M. M. Pejović and R. D. Filipović *Int. J. Electron.* **67** (1989) 251.
18. S. Dushman, *Scientific Foundations of Vacuum Technique*, John Wiley, New York (1949).
19. L.B. Loeb, *Basic Processes of Gaseous Electronics*, University of California Press, Berkley (1961).
20. Dj. A. Bošan and M.M. Pejović, *J. Phys. D: Appl. Phys.* **12** (1979) 1699
21. M. M. Pejović, G.S. Ristić, Č. S. Milosavljević, P. Vuković and J.P. Karamarković, VACUUM - Surface Engin., Surface Instrum. and Vacuum Technol. **53** (1999) 435.
22. M. J. Meek and D. J. Craggs, *Electrical breakdown of gasses*, Wiley, Chichester, UK (1978)
23. J. P. Karamarković, G. S. Ristić and M. M. Pejović, presented at *BPU₄*, Veliko Trunovo, (Bulgaria), to be printed
24. von Laue, *Ann. Phys.* **76** (1925) 721
25. V. Lj. Marković, (1994) 8514
26. A. von Engel, *Ionized Gases*, Clarendon Press, Oxford (1965).
27. M. M. Pejović, G. S. Ristić and Z. Lj. Petrović, *J. Phys. D: Appl. Phys.* **32** (1999) 1489.
28. Dj. A. Bošan, T. V. Jovanović and Dj. M. Krmpotić, *J. Phys. D: Appl. Phys.* **30** (1997) 3096.
29. T. V. Jovanović, Dj. A. Bošan and Dj. M. Krmpotić, *J. Phys. D: Appl. Phys.*, **31** (1998) 3249
30. M. M. Pejović and Dj. A. Bošan, *J. Phys. D: Appl. Phys.*, **14** (1981) 693
31. V. S. Fomenko, *Emissionnye svoystva materialov, Spravochnik*, Naukova Dumka, Kiev (1970).
32. M. M. Pejović and B. Dimitrijević, *J. Phys. D: Appl. Phys.* **15** (1982) 87.
33. V. Lj. Marković, Z. Lj. Petrović and M. M. Pejović, *Jpn. J. Appl. Phys.* **34** (1995) 2466.
34. M. M. Pejović, V. Lj. Marković, G. S. Ristić and S. Mekić, *IEE Proc.-Sci. Meas. Technol.* **143** (1996) 413.
35. J. Berkowitz, W. A. Chupka and G. B. Kristiakowsky, *J. Chem. Phys.* **25** (1956) 457.
36. R. A. Young and G. A. John St., *J. Chem. Phys.* **48** (1968) 895 .
37. G. N. Hays and H. J. Oskam, *J. Chem. Phys.* **59** (1973) 1507.
38. G. N. Hays and H. J. Oskam, *J. Chem. Phys.* **59** (1973) 6088.
39. T. Makabe, H. Awai and T. Mori, *J. Phys. D: Appl. Phys.* **17** (1984) 2368.
40. L. G. Piper, *J. Chem. Phys.* **90** (1989) 7087.
41. V. Lj. Marković, M. M. Pejović and Z. Lj. Petrović, *J. Phys. D: Appl. Phys.* **26** (1993) 1611.
42. W. Brennen and C. E. Shone, *J. Chem. Phys.* **75** (1971) 1552.
43. Phelps A V , personal communication.
44. M. M. Pejović, V. Lj. Marković, G. S. Ristić, S. I. Mekić, *Vacuum - Surface Engin, Surface instr. and vacuum technology* **48** (1997) 531.
45. G. N. Hays, C. J. Trasy and H. J. Oskam, *J. Chem. Phys.* **60** (1974) 2074.
46. R.S. Van Dyck, C.E. Johnson and H.A. Shugort, *Phys. Rev. A* **5** (1972) 991
47. N. E. Small-Warren and L. Y. Schow Chin, *Phys. Rev. A* **11** (1975) 1777.
48. M. M. Pejović and G. S. Ristić, submitted to *Plasma Sci. Technol.*
49. Y. Ichikawa and S. Teii *J. Phys. D: Appl. Phys.* **13** (1980) 2031.

VREME KAŠNJENJA ELEKTRIČNOG PROBOJA U GASOVIMA NA NISKIM PRITISCIMA

Momčilo Pejović, Goran S. Ristić, Jugoslav P. Karamarković

U ovom radu je prikazan pregled naših istraživanja vremena kašnjenja električnog proboja u gasovima na niskim pritiscima. Izvršena je statistička analiza korišćenjem Laue-ovih raspodela i histograma eksperimentalno dobijenih podataka. Razmatran je uticaj raznih parametara (prenapona, temperature i materijala katode, struje pražnjenja) na vreme kašnjenja. Razmatrane su memorijske krive i njihova primena za procenu vremena rekombinacije pozitivnih jona, vremena katalitičke rekombinacije atoma azota kao i vremena deekscitacije metastabilnih stanja u kriptonu.